

A priori estimates on the partial realized gain of UWB-antennas

Christian Sohl and Mats Gustafsson

Dept. of Electrical and Information Technology, Lund University, P.O. Box 118, S-211 00 Lund, Sweden.
{Christian.Sohl, Mats.Gustafsson}@eit.lth.se; fax +46-46 12 99 48.

Abstract

A summation rule valid for a large class of linear and reciprocal antennas is presented in terms of the electric and magnetic polarizability dyadics. The identity is based on the holomorphic properties of the forward scattering dyadic and includes arbitrary shaped antennas modeled by linear and time-translational invariant constitutive relations. In particular, a priori estimates on the partial realized gain are introduced, and lower bounds on the onset frequency is derived for two important archetypes of UWB-antennas. The theoretical findings are illustrated by the equiangular planar spiral antenna, and comparison with numerical simulations show great potential for future use in antenna theory.

1 Introduction

Since the pioneering ideas in Refs. 1 and 2 more than half a century ago, a priori bounds on the directivity and the Q -factor of electrically small antennas have attracted great attention in the scientific community. Unfortunately, the results by Chu and Wheeler, and many of the subsequent papers discussed in Ref. 3, not only overestimate the true antenna performance, but also show severe restrictions such as the lack of any material description and polarization dependence. To overcome these imperfections, a new set of isoperimetric bounds are introduced in Refs. 4 and 5 that apply to a large class of linear and reciprocal antennas. These new bounds are based on the principles of causality and power conservation rather than the traditional approach using the spherical vector waves. Another drawback of the classical formulation is due to the difficulty of extending the spherical vector waves to accurately model the electromagnetic field inside the smallest circumscribing sphere.

The classical bounds also show severe restrictions with respect to the electrical size of the investigated antenna. Due to the assumption of a dominant lowest order spherical vector mode, the classical bounds only hold for electrically small and resonant antennas. As far as the authors know, no similar bounds to Chu and Wheeler exist in the literature for non-resonant antennas with a broadband partial realized gain. Since UWB-antennas show great potential for future applications in stealth technology, radar imaging and precision positioning, it is of scientific importance to develop an insight into the underlying limitations of such antennas [6].

2 A summation rule for the partial realized gain

This paper is based on a recent antenna theory set forth in Refs. 4 and 5. For this purpose, consider an antenna of arbitrary shape modeled by linear and time-translational invariant constitutive relations in terms of the electric and magnetic susceptibilities, $\chi_e = \chi_e(\mathbf{x})$ and $\chi_m = \chi_m(\mathbf{x})$, respectively.¹ Based on the holomorphic properties of the forward scattering dyadic, a summation rule for the partial realized gain g (with respect to the $\hat{\mathbf{k}}$ -direction in space and the $\hat{\mathbf{e}}$ -polarization of the radiated electric field) is derived in Refs. 4 and 5, *viz.*,

$$\int_0^\infty \frac{g(k; \hat{\mathbf{k}}, \hat{\mathbf{e}})}{k^4} dk = \frac{\eta(-\hat{\mathbf{k}}, \hat{\mathbf{e}}^*)}{2} \left(\hat{\mathbf{e}}^* \cdot \boldsymbol{\gamma}(\chi_e) \cdot \hat{\mathbf{e}} + (\hat{\mathbf{k}} \times \hat{\mathbf{e}}^*) \cdot \boldsymbol{\gamma}(\chi_m) \cdot (\hat{\mathbf{k}} \times \hat{\mathbf{e}}) \right), \quad (1)$$

where $k \in [0, \infty)$ denotes the wave number in free space, and the generalized absorption efficiency $\eta \in [0, 1)$ is determined from the overall scattering properties of the antenna. Here, the static polarizability dyadic $\boldsymbol{\gamma}$ is defined by ($\ell = e, m$ depending on whether the problem is of electric ($\ell = e$) or magnetic ($\ell = m$) nature)

$$\boldsymbol{\gamma}(\chi_\ell) = \sum_{i,j=1}^3 \left(\hat{\mathbf{a}}_i \cdot \iiint_{\mathbb{R}^3} \chi_\ell(\mathbf{x}) (\hat{\mathbf{a}}_j - \nabla \psi_j(\mathbf{x})) dV \right) \hat{\mathbf{a}}_i \hat{\mathbf{a}}_j, \quad (2)$$

¹The results in this paper are formulated for isotropic susceptibilities but can easily be modified to include bi-anisotropic effects.

where the unit vectors $\hat{\mathbf{a}}_1$, $\hat{\mathbf{a}}_2$ and $\hat{\mathbf{a}}_3$ are assumed to be linearly independent. The scalar potential ψ_j is the unique solution to the exterior problem

$$\begin{cases} \nabla \cdot ((\chi_\ell(\mathbf{x}) + 1)\nabla\psi_j(\mathbf{x})) = \hat{\mathbf{a}}_j \cdot \nabla\chi_\ell(\mathbf{x}) \\ \psi_j(\mathbf{x}) = \mathcal{O}(x^{-2}) \text{ as } x \rightarrow \infty \end{cases} \quad \mathbf{x} \in \mathbb{R}^3, \quad (3)$$

where $x = |\mathbf{x}|$. In terms of (1), it is intriguing to note that an antenna's overall dynamical properties is directly related to its static or low-frequency response.

As an example of how this summation rule can be used in modern antenna design, consider an arbitrary antenna Λ enclosed by a circular disk $\Lambda_+ = \{\mathbf{x} \in \mathbb{R}^3 : x \leq a\}$ of radius a .² Let $\hat{\nu}$ denote the outward-directed unit normal vector, and choose $\hat{\mathbf{k}} = \hat{\nu}$ and $\hat{\mathbf{e}} = \hat{\rho}$, corresponding to a direction of observation and an electric polarization perpendicular and parallel to the disk, respectively. Introduce the frequency band [3.1, 10.6] GHz (or, equivalently, the wave number interval [0.65, 2.22] cm^{-1}) as the appropriate frequency band for UWB-communication in North America. Assume that Λ is specified to have a partial realized gain g satisfying

$$g(k; \hat{\nu}, \hat{\rho}) \geq \begin{cases} g_{\text{level}}(\hat{\nu}, \hat{\rho})k^4/k_1^4 & k \in [0, k_1] \\ g_{\text{level}}(\hat{\nu}, \hat{\rho}) & k \in [k_1, k_2] \\ 0 & \text{otherwise} \end{cases}, \quad (4)$$

where $k_1 = 0.65 \text{ cm}^{-1}$ and $k_2 = 2.22 \text{ cm}^{-1}$. Then, for a given threshold g_{level} , it is desirable to determine the smallest radius a such that the partial realized gain of Λ fulfills the above-stated requirements.

Based on (4), the left hand side of (1) is estimated from below by

$$\int_0^\infty \frac{g(k; \hat{\nu}, \hat{\rho})}{k^4} dk \geq g_{\text{level}}(\hat{\nu}, \hat{\rho}) \left(\frac{1}{k_1^3} + \int_{k_1}^{k_2} \frac{dk}{k^4} \right) = \frac{g_{\text{level}}(\hat{\nu}, \hat{\rho})}{3} \frac{4k_2^3 - k_1^3}{k_1^3 k_2^3}. \quad (5)$$

From the analysis in Ref. 4, it follows that the polarizability dyadics for the perfectly electric conducting disk are $\gamma(\chi_e) = 16a^3 \mathbf{I}_\perp / 3$ and $\gamma(\chi_m) = \mathbf{0}$, respectively, where $\mathbf{I}_\perp = \mathbf{I} - \hat{\nu}\hat{\nu}$ denotes the projection dyadic in \mathbb{R}^3 . Hence, by inserting (5) into (1), one obtains

$$\frac{g_{\text{level}}(\hat{\nu}, \hat{\rho})}{a^3} \leq 0.55\eta(-\hat{\nu}, \hat{\rho}), \quad (6)$$

where a now measures the radius of the disk in units of cm. For example, by invoking the bound $\eta < 1$, it is concluded that the minimum radius of the disk is 1.8 cm for $g_{\text{level}} = 3$ and 1.9 cm for $g_{\text{level}} = 4$. For many antennas, η is close to 1/2 and a more realistic bound is therefore 2.2 cm and 2.4 cm for $g_{\text{level}} = 3$ and $g_{\text{level}} = 4$, respectively.

3 A priori estimates on UWB-antennas

A priori estimates for two archetypes of UWB-antennas are presented in this section, *viz.*, antennas characterized by a constant partial realized gain and antennas characterized by a constant effective antenna aperture.

3.1 Constant partial realized gain $g_p(\hat{\mathbf{k}}, \hat{\mathbf{e}})$

Due to the non-negative character of the partial realized gain, the left hand side of (1) can be estimated from below by integrating over $K = [k_p, \infty)$ rather than the positive real axis. Thus, a straightforward calculation using the threshold $g_p(\hat{\mathbf{k}}, \hat{\mathbf{e}}) = \min_{k \in K} g(k; \hat{\mathbf{k}}, \hat{\mathbf{e}})$ yields

$$\int_0^\infty \frac{g(k; \hat{\mathbf{k}}, \hat{\mathbf{e}})}{k^4} dk \geq g_p(\hat{\mathbf{k}}, \hat{\mathbf{e}}) \int_K \frac{dk}{k^4} = \frac{g_p(\hat{\mathbf{k}}, \hat{\mathbf{e}})}{3k_p^3}. \quad (7)$$

²Here, the antenna support is defined by $\Lambda = \Lambda_e \cup \Lambda_m$, where $\Lambda_\ell = \{\mathbf{x} \in \mathbb{R}^3 : \chi_\ell(\mathbf{x}) \neq 0\}$.

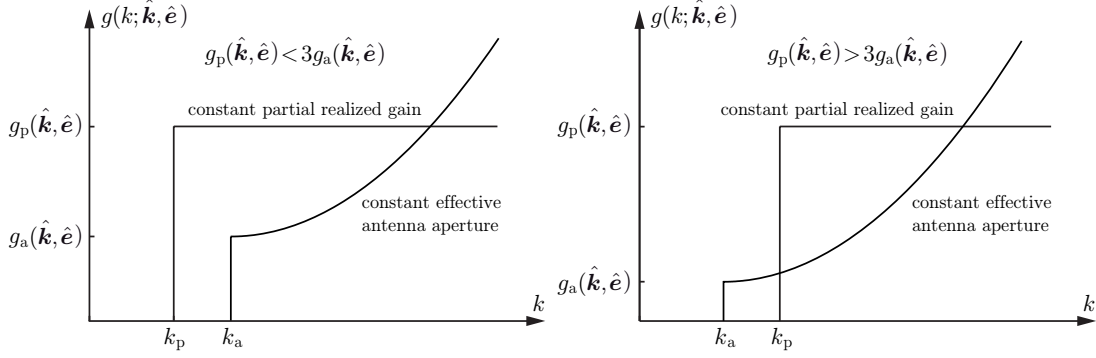


Figure 1: A comparison between a priori estimates for a constant partial realized gain, $g_p(\hat{\mathbf{k}}, \hat{\mathbf{e}})$, and a constant effective antenna aperture, $\pi g_a(\hat{\mathbf{k}}, \hat{\mathbf{e}})/k_a^2$.

Combining this estimate with (1) implies that

$$\frac{g_p(\hat{\mathbf{k}}, \hat{\mathbf{e}})}{3k_p^3} \leq \frac{\eta(-\hat{\mathbf{k}}, \hat{\mathbf{e}}^*)}{2} \left(\hat{\mathbf{e}}^* \cdot \boldsymbol{\gamma}(\chi_e) \cdot \hat{\mathbf{e}} + (\hat{\mathbf{k}} \times \hat{\mathbf{e}}^*) \cdot \boldsymbol{\gamma}(\chi_m) \cdot (\hat{\mathbf{k}} \times \hat{\mathbf{e}}) \right), \quad (8)$$

with equality if and only if $g(k; \hat{\mathbf{k}}, \hat{\mathbf{e}}) = g_p(\hat{\mathbf{k}}, \hat{\mathbf{e}})$ for $k \in [k_p, \infty)$, and zero elsewhere. The interpretation of (8) is that it yields a lower bound on the onset frequency k_p , or, equivalently, an upper bound on the threshold $g_p(\hat{\mathbf{k}}, \hat{\mathbf{e}})$, in terms of the antenna geometry and its static material parameters. From a physical point of view, an antenna with a constant partial realized gain is characterized by receiving less power as frequency increases since the effective antenna aperture then varies inversely with the square of the frequency.

3.2 Constant effective antenna aperture $\pi g_a(\hat{\mathbf{k}}, \hat{\mathbf{e}})/k_a^2$

A constant effective antenna aperture implies that the partial realized gain varies with the square of the frequency. For this purpose, introduce the constant effective antenna aperture $\pi g_a(\hat{\mathbf{k}}, \hat{\mathbf{e}})/k_a^2$, corresponding to the threshold $g_a(\hat{\mathbf{k}}, \hat{\mathbf{e}}) = k_a^2 \min_{k \in K} g(k; \hat{\mathbf{k}}, \hat{\mathbf{e}})/k^2$, where the wave number interval K now is defined as $K = [k_a, \infty)$. Then, analogous to (8), it is concluded that

$$\frac{g_a(\hat{\mathbf{k}}, \hat{\mathbf{e}})}{k_a^3} \leq \frac{\eta(-\hat{\mathbf{k}}, \hat{\mathbf{e}}^*)}{2} \left(\hat{\mathbf{e}}^* \cdot \boldsymbol{\gamma}(\chi_e) \cdot \hat{\mathbf{e}} + (\hat{\mathbf{k}} \times \hat{\mathbf{e}}^*) \cdot \boldsymbol{\gamma}(\chi_m) \cdot (\hat{\mathbf{k}} \times \hat{\mathbf{e}}) \right), \quad (9)$$

with equality if and only if $g(k; \hat{\mathbf{k}}, \hat{\mathbf{e}}) = g_a(\hat{\mathbf{k}}, \hat{\mathbf{e}})k^2/k_a^2$ for $k \in [k_a, \infty)$, and zero elsewhere.

For a given right hand side of (1), a comparison between (8) and (9) shows that the onset frequencies k_p and k_a satisfy $k_p/k_a = (g_p(\hat{\mathbf{k}}, \hat{\mathbf{e}})/3g_a(\hat{\mathbf{k}}, \hat{\mathbf{e}}))^{1/3}$, implying that $k_p > k_a$ for $g_p(\hat{\mathbf{k}}, \hat{\mathbf{e}}) > 3g_a(\hat{\mathbf{k}}, \hat{\mathbf{e}})$, and $k_p < k_a$ for $g_p(\hat{\mathbf{k}}, \hat{\mathbf{e}}) < 3g_a(\hat{\mathbf{k}}, \hat{\mathbf{e}})$. This conclusion is illustrated in Fig. 1 using the following models with identical values of (1): $g(k; \hat{\mathbf{k}}, \hat{\mathbf{e}}) = g_p(\hat{\mathbf{k}}, \hat{\mathbf{e}})$ for $k \in [k_p, \infty)$, and $g(k; \hat{\mathbf{k}}, \hat{\mathbf{e}}) = g_a(\hat{\mathbf{k}}, \hat{\mathbf{e}})k^2/k_a^2$ for $k \in [k_a, \infty)$, and zero elsewhere. In particular, $g_p(\hat{\mathbf{k}}, \hat{\mathbf{e}}) < 3g_a(\hat{\mathbf{k}}, \hat{\mathbf{e}})$ and $g_p(\hat{\mathbf{k}}, \hat{\mathbf{e}}) > 3g_a(\hat{\mathbf{k}}, \hat{\mathbf{e}})$ in Fig. 1 refer to $k_p < k_a$ and $k_p > k_a$, respectively. Although it is seems unphysical to include infinite high frequencies in (8) and (9), it is not a severe restriction since the damping factor $1/k^4$ on the left hand side of (1) implies that the integral mainly is dominated by the antenna's low- and intermediate frequency behavior.

4 A numerical example: the equiangular planar spiral antenna

A numerical simulation using the method of moments is employed to illustrate the estimates in Sec. 3 for the equiangular planar spiral antenna depicted in Fig. 2. The maximum gain, $G_{\max}(k) = \max_{\hat{\mathbf{k}}, \hat{\mathbf{e}}=0} G(k; \hat{\mathbf{k}}, \hat{\mathbf{e}})$, the partial gain

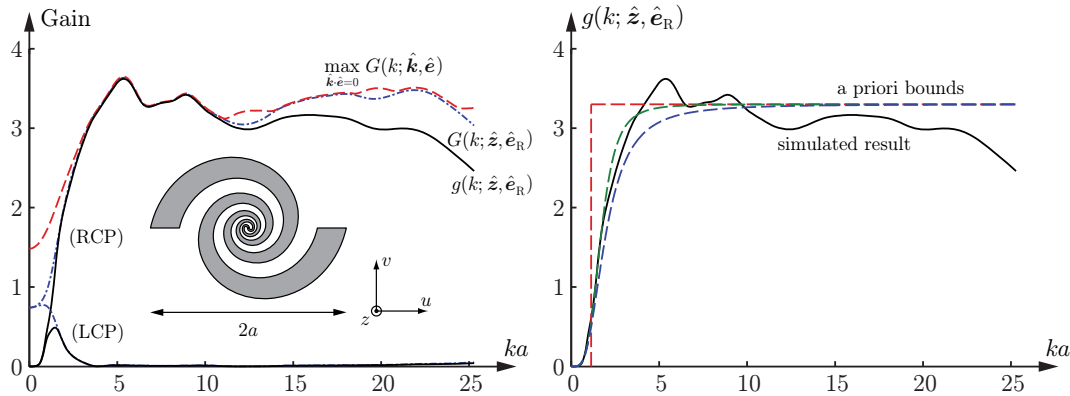


Figure 2: Left figure: maximum gain (red dashed line), partial gain (blue dashed-dotted line), and partial realized gain (black solid line) for both the RCP- and the LCP-polarizations. Right figure: a priori estimates of the partial realized gain derived from the electrostatic properties of the antenna using (8).

$G(k; \hat{z}, \cdot)$ in the positive \hat{z} -direction, and the partial realized gain $g(k; \hat{z}, \cdot)$ in the positive \hat{z} -direction are depicted on the left hand side of Fig. 2. It is observed that the antenna is right circularly polarized (RCP) with an approximately constant partial realized gain in the \hat{z} -direction. For comparison, the corresponding curves for the left circularly polarized (LCP) radiation are included in Fig. 2 with an overall partial realized gain less than unity. The dashed lines on the right hand side of Fig. 2 are derived by solving (2) and (3) in the perfectly electric conducting limit. All three estimates on the right hand side of Fig. 2 are seen to model the overall frequency characteristics of the antenna remarkably well. These bounds should also be compared with the corresponding result (6) for the smallest circumscribing disk.

5 Conclusions

Although the electric and magnetic polarizability dyadics are restricted to the static or low-frequency regime, the above-mentioned examples suggest that the polarizability dyadics are crucial for the understanding of an antenna's ability to direct energy over a frequency interval. A striking consequence of (2) and (3) is that the interior of an antenna has less influence on the polarizability dyadic compared with its boundary surface. Removing interior parts of the antenna will only slightly reduce (1) but mainly redistribute the integrand along the frequency axis. Thus, it is concluded that the analysis presented in this paper reproduces the well-known rule of thumb that the boundary is the critical parameter in antenna design, far more so than the antenna's surface area or interior geometry.

References

- [1] L. J. Chu. "Physical limitations of omni-directional antennas". *Appl. Phys.*, vol. 19, pp. 1163–1175, 1948.
- [2] H. A. Wheeler. "Fundamental limitations of small antennas". *Proc. IRE*, vol. 35(12), pp. 1479–1484, 1947.
- [3] R. C. Hansen. *Electrically small, superdirective, and superconductive antennas*. New Jersey: John Wiley & Sons, 2006.
- [4] M. Gustafsson, C. Sohl, and G. Kristensson. "Physical limitations on antennas of arbitrary shape". *Proc. R. Soc. A*, vol. 463, pp. 2589–2607, 2007.
- [5] C. Sohl, M. Gustafsson, and G. Kristensson. "An introduction to isoperimetric bounds on antennas". Tech. Rep. LUTEDX/(TEAT-7157)/1–9/(2007), Lund University, Department of Electrical and Information Technology, P.O. Box 118, S-221 00 Lund, Sweden, 2007.
- [6] H. Schantz. *The Art and Science of Ultrawideband Antennas*. Boston, London: Artech House, 2005.